Electron trapping around a magnetic null

J.-S. He,[1] Q.-G. Zong,[1,2] X.-H. Deng,[3] C.-Y. Tu,[1] C.-J. Xiao,[4] X.-G. Wang,[5] Z.-W. Ma,[6] Z.-Y. Pu,[1] E. Lucek,[7] A. Pedersen,[8] A. Fazakerley,[9] N. Cornilleau-Wehrlin,[10] M. W. Dunlop,[11] H. Tian,[1] S. Yao,[1] B. Tan,[1] S.-Y. Fu,[1] K.-H. Glassmeier,[12] H. Reme,[13] I. Dandouras,[13] and C. P. Escoubet[14]

Received 22 March 2008; accepted 2 May 2008; published 29 July 2008.

[1] Magnetic reconnection is an important process in astrophysical, space and laboratory plasmas. The magnetic null pair structure is theoretically suggested to be a crucial feature of the three-dimensional magnetic reconnection. The physics around the null pair, however, has not been explored in combination with the magnetic field configuration deduced from in situ observations. Here, we report the identification of the configuration around a null pair and simultaneous electron dynamics near one null of the pair, observed by four Cluster spacecraft in the geo-magnetotail. Further, we propose a new scenario of electron dynamics in the null region, suggesting that electrons are temporarily trapped in the central reconnection region including electron diffusion region resulting in an electron density peak, accelerated possibly by parallel electric field and electron pressure gradient, and reflected from the magnetic cusp mirrors leading to the bi-directional energetic electron beams, which excite the observed high frequency electrostatic waves. **Citation:** He, J.-S., et al. (2008), Electron trapping around a magnetic null, *Geophys. Res. Lett.*, *35*, L14104, doi:10.1029/2008GL034085.

1. Introduction

[2] The nature of a magnetic null pair in a magnetic reconnection region has two intrinsic interconnected aspects: geometry and dynamics. Theoretical studies on the null pair geometry indicate that magnetic field lines close to a null have two distinct parts: a spine, where the field lines are bunched together, and a fan, where the field lines are distributed apart from each other [*Dungey*, 1963; *Cowley*, 1973; *Greene*, 1988; *Lau and Finn*, 1990; *Priest and Titov*, 1996; *Priest and Forbes*, 2000; *Dorelli et al.*, 2007]. An isolated null in the geo-magnetosphere was identified using a topological degree method of *Greene* [1992] by *Xiao et al.* [2006] and extrapolation with a non-linear fitting function by *He et al.* [2008]. Characteristics of two nulls identified respectively at two different time instances were combined to infer that of a null pair under the assumption that the null identified first remains unchanged till the second null was observed [*Xiao et al.*, 2007]. However no field line configuration of a null pair has yet been identified from simultaneous in situ measurements.

[3] On the other hand, the canonical picture of the dynamics of magnetic reconnection in collisionless plasmas is usually described, according to different scale lengths, with respect to three physically distinguishable regions nested from the outside of the current sheet to the center of the reconnection site, called as ideal magnetohydrodynamic region, ion diffusion region, and electron diffusion region respectively [*Vasyliunas*, 1975]. This theoretical picture was tested by numerical simulations [*Birn et al.*, 2001; *Ricci et al.*, 2004; *Fujimoto*, 2006; *Karimabadi et al.*, 2007] and compared with gradually revealed observational evidences occurring in various length scales [*Øieroset et al.*, 2001; *Deng and Matsumoto*, 2001; *Mozer et al.*, 2002; *Vaivads et al.*, 2004; *Egedal et al.*, 2005].

[4] Certain aspects of electron dynamics near the reconnection region mostly in the two-dimensional (2-D) frame were discussed [e.g., *Karimabadi et al.*, 2007; *Mozer et al.*, 2002; *Egedal et al.*, 2005; *Henderson et al.*, 2006]. Electrons are predicted by 2-D simulation to be temporarily trapped in the inner electron diffusion region [*Karimabadi et al.*, 2007]. The electron trapping in the ion diffusion region was theoretically demonstrated to result from the accumulated-ion-established electrostatic potential plus the magnetic cusp geometry, and was used to explain the observed anisotropic electron velocity distribution [*Egedal et al.*, 2005]. Nevertheless, the electron dynamics in the electron diffusion region, especially associated with a 3-D magnetic null pair, has not yet been addressed observationally.

[5] In this letter, we present results of both the geometry and dynamical physics around a magnetic null pair from in situ measurements by four identical Cluster satellites [*Escoubet et al.*, 2001]. The results shed new light on the inner region physics of 3-D reconnection. The electron density peak, detected in the central reconnection region including electron diffusion region around the null may represent electrons temporarily trapped in the small scale

[1]School of Earth and Space Sciences, Peking University, Beijing, China.
[2]Center for Atmospheric Research, University of Massachusetts Lowell, Lowell, Massachusetts, USA.
[3]Department of Space Physics, Wuhan University, Wuhan, China.
[4]National Astronomical Observatories, Chinese Academy of Sciences, Beijing, China.
[5]School of Physics, Peking University, Beijing, China.
[6]Institute for Fusion Theory and Simulation, Zhejiang University, Hangzhou, China.
[7]Space and Atmospheric Physics, Imperial College, London, UK.
[8]Department of Physics, University of Oslo, Blindern, Oslo, Norway.
[9]Department of Space and Climate Physics, Mullard Space Science Laboratory, University College London, Dorking, UK.
[10]CETP, CNRS, Velizy, France.
[11]Space Sciences Division, SSTD, Rutherford Appleton Laboratory, Chilton, UK.
[12]Institut für Geophysik und Meteorologie, Technische Universität Braunschweig, Braunschweig, Germany.
[13]Centre d'Etude Spatiale des Rayonnements, Toulouse, France.
[14]ESTEC, ESA, Noordwijk, Netherlands.

0094-8276/08/2008GL034085

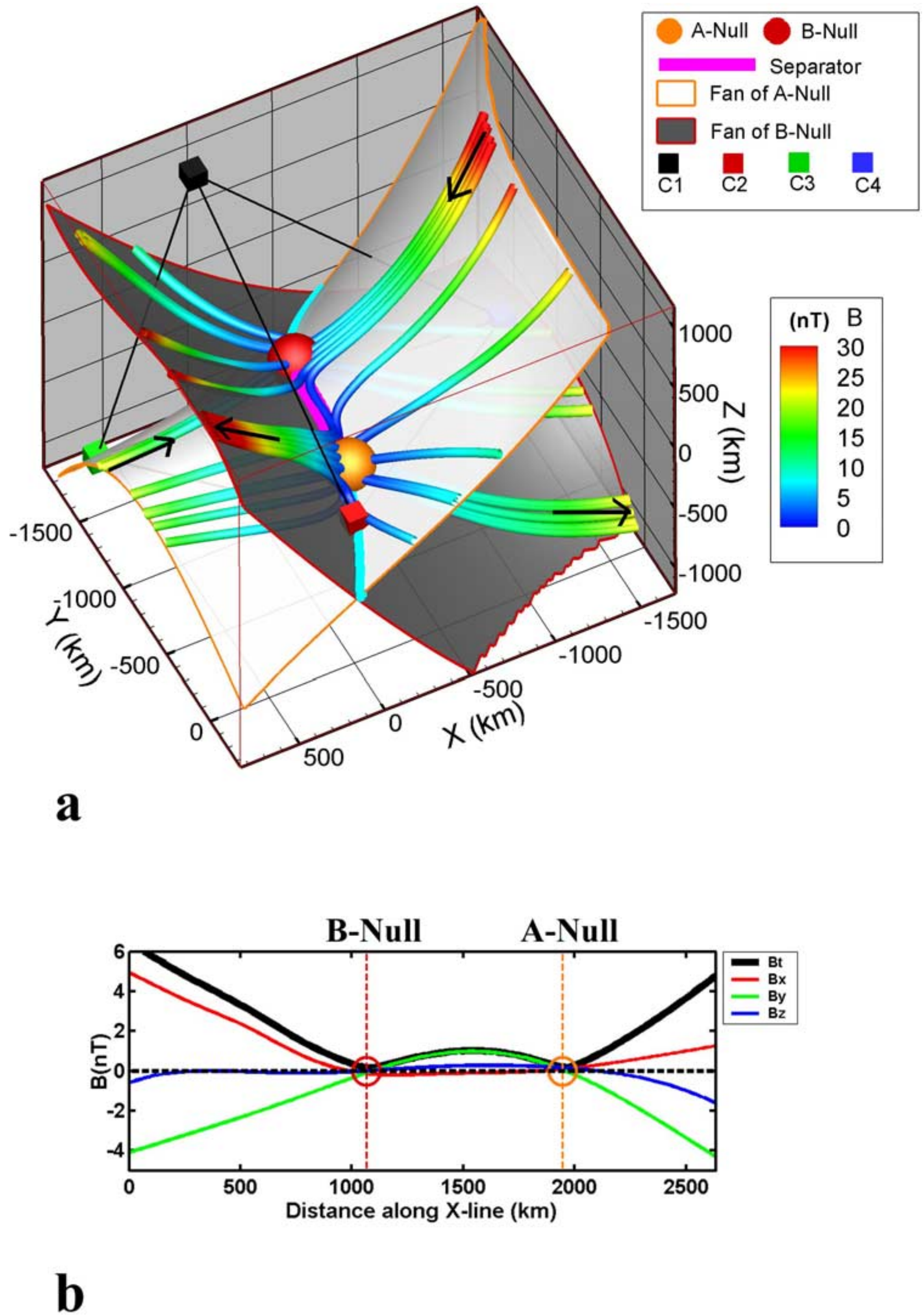

Figure 1. Magnetic field configuration of a magnetic null pair reconstructed from Cluster measurements when Cluster C2 crosses the neutral sheet. (a) Separator reconnection configuration reconstructed from observations by Cluster at 09:48:25.637. A-null and B-null are shown as orange and red balls, respectively, with the separator as a bold pink curve connecting them. Magnetic field lines colored by local field strengths converge along the fan surface (in white) to approach the A-null and then travel out along the spine (marked in black arrows) of the A-null. Magnetic field lines converge along the spine of the B-null and then diverge out along its fan surface (in grey). Cluster C1, C2, C3, C4 are drawn as four cubes in black, red, green, and blue, respectively. The origin of the illustrating coordinates is at the C2 position. (b) Magnetic field strength distributed on the X-line. The total field strength is drawn in bold black. Three components, B_x, B_y, and B_z, are in red, green and blue, respectively. The x-coordinate is the distance along X-line starting at the beginning with the smallest y in Figure 1a. The orange (red) circle marks the location of the A-null (B-null).

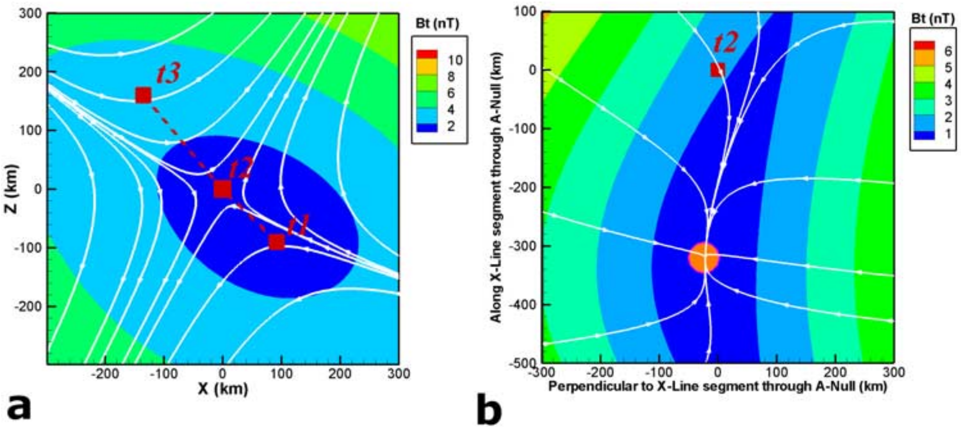

Figure 2. Cluster C2 positions on 2-D cross-sections of the magnetic field configuration when C2 observes the enhancement of electron number density.The white lines show the 2-D projection of the 3-D field line vector. (a) C2 positions, marked by the red rectangles on top of the regions with different total magnetic field strength Bt, with its strength shown by the color contour and in the color bar, on the GSM x−z plane, at the time sequences of *t*1=09:48:25.548 UT, *t*2=09:48:25.637 UT, and *t*3=09:48:25.726 UT. The B_t distribution and field lines are reconstructed from data at *t*2. (b) The other 2-D cross-section of the magnetic field configuration at the time *t*2, passing through the C2 position and a segment of X-line with the A-null on it. Magnetic field lines traced in this 2-D plane are drawn as white lines on it, appearing to be converging to the A-null (the orange ball).

magnetic cavity. The trapped electrons are likely to be accelerated by parallel electric field and electron pressure gradient from a Hall MHD point of view, and bounced between the magnetic cusps characterized with observed bi-directional energetic electron beams. The electron beam instability produces the high frequency electrostatic waves, scattering the trapped energetic electrons to escape from the loss cone.

2. Analysis of Cluster Measurements

[6] The measurements by various payloads on Cluster, e.g., FGM [*Balogh et al.*, 2001], EFW [*Gustafsson et al.*, 2001], PEACE [*Johnstone et al.*, 1997], STAFF [*Cornilleau-Wehrlin et al.*, 2003], and CIS [*Rème et al.*, 2001] are used in this study. The Cluster array encountered an active magnetic reconnection site in the geo-magnetotail over a period from 09:40:00 to 09:55:00 UT on Oct 1st 2001 [*Runov et al.*, 2003; *Wygant et al.*, 2005; *Cattell et al.*, 2005; *Xiao et al.*, 2007; *Imada et al.*, 2007; *Chen et al.*, 2007]. Spacecraft C2 passed through a thick current layer during a time interval from 09:48:17 to 09:48:40 UT (23 sec) and a thin current layer embedded in it from 09:48:25.000 to 09:48:25.800 UT (0.8 sec). At about 09:48:25.637 UT, C2 crossed the neutral sheet with B_x component in GSM changing from negative to positive to provide a good opportunity for focusing on the plasma dynamics across the neutral sheet.

[7] To set up the stage for dynamics study, we reconstruct the magnetic reconnection configuration from the four magnetic field vectors, simultaneously measured by all four Cluster satellites, making use of a novel extrapolation of magnetic field [*He et al.*, 2008] (see auxiliary materials).[1] It should be pointed out that no Hall-current is considered in the field extrapolation method, because the Hall-currents locate outside the extrapolation box according to *Runov et al.* [2003], who showed that the Hall-currents locate at both ends of a long current sheet crossing through the extrapolation region. The magnetic field configuration around a magnetic null pair reconstructed from the Cluster measurements at 09:48:25.637 UT is shown in Figure 1a. Clearly, Cluster encountered a typical separator reconnection configuration [*Priest and Forbes*, 2000]. A pair of magnetic nulls, with the separator connecting them, is encompassed by the Cluster tetrahedron. Furthermore, Cluster C2 is located nearly on the X-line extending the separator from the A-null. The distance between C2 and the A-null can be estimated as 385 km, less than the ion inertial length of 1853 km and on the order of the ‘‘ion acoustic’’ gyro-radius of 374 km (see AM). The distance between C2 and the X-line however is about 50 km, on the order of the electron inertial length of 43 km (see AM). The event thus places C2 in the electron dynamics region, considering that uncertainty of the extrapolation in this case is of the order of 10 km. However, it could be said conservatively that C2 was located in the central reconnection region including electron diffusion region. The reconnection rate of this event is estimated to be $0.08V_A$, based on C1 observation of southward plasma flow in the northern lobe region (Figure 1a).

[8] Figure 1b illustrates the variation of the magnetic field strength on the X-line. The magnitude of the magnetic field components become zero at the positions of the nulls. On the separator between the nulls, the Y-component of the magnetic field dominates over the other two and represents the so-called guide field on the separator. The small guide field with a maximum of 1 nT implies a weak guide field effect on the reconnection rate [*Ricci et al.*, 2004]. The length of the separator is about 880 km.

[9] We also reconstruct the reconnection configuration before and after 09:48:25.637 to obtain an overview of the satellite motion in this frame. As seen in Figure 2a (GSM x−z plane) C2 moves upward to approach the 2-D X-point from the southern earthward magnetic cusp, passes

[1]Auxiliary materials are available in the HTML. doi:10.1029/2008GL034085.

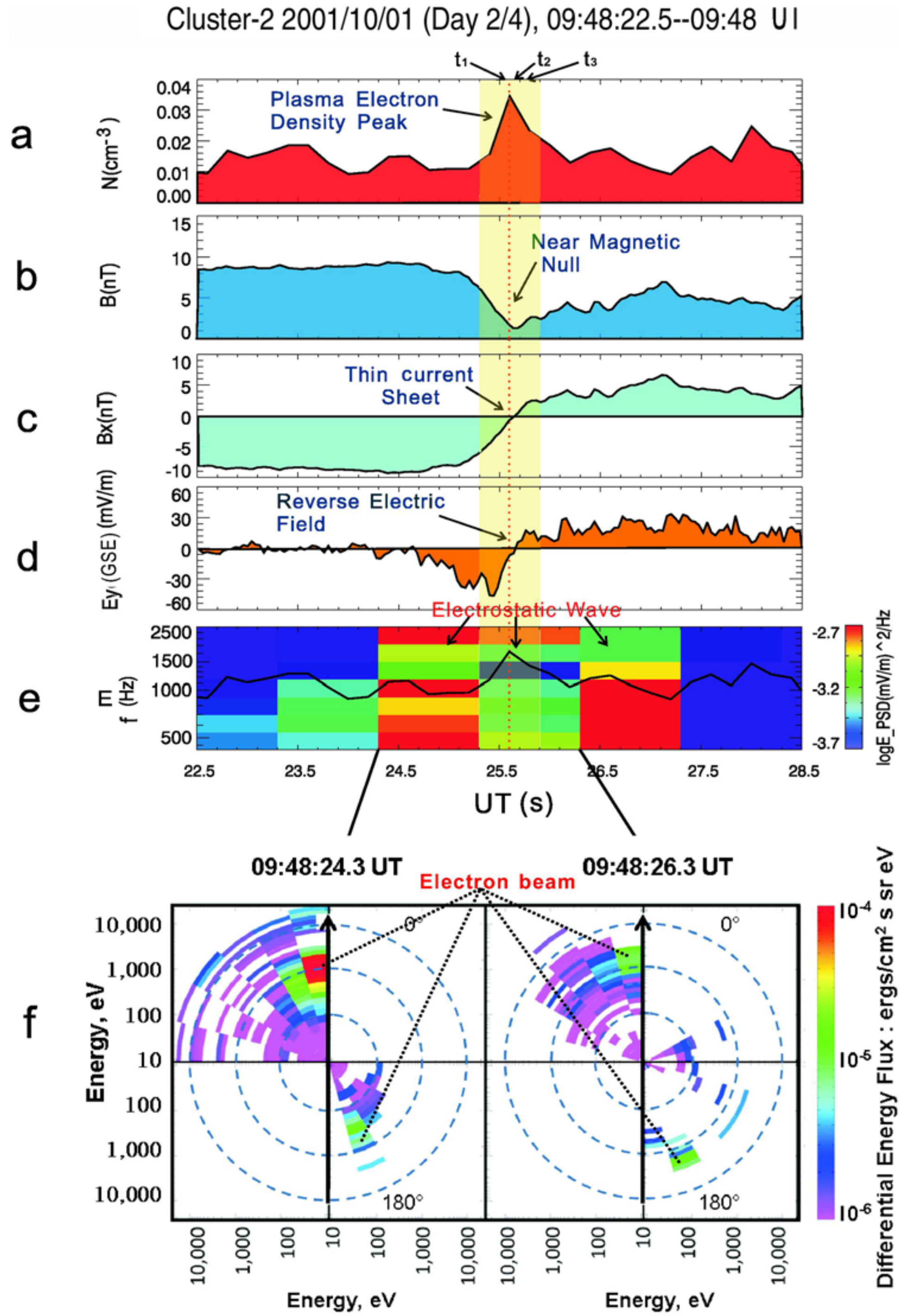

Figure 3. Observations by Cluster C2 over the period from 09:48:22.5 to 09:48:28.5 UT. (a) The plasma electron number density inferred from potential measurements by EFW. (b) The total magnetic field strength measured by FGM. (c) The magnetic field component of B_x measured by FGM in GSM. (d) The electric field component of E_y measured by EFW in GSE. (e) The electric field wave power spectrum observed by STAFF. The black line denotes the electron plasma frequency. (f) Two pitch angle distributions (PAD) of electron differential energy flux density measured by PEACE at 09:48:24.3 and 09:48:26.3 UT, respectively measured in a 1/8 sec interval. The orange dotted vertical line through Figure 3 a–e is located at the time of 09:48:25.6 UT.

through the X-point at 09:48:25.637 UT, and then moves away to the northern tailward magnetic cusp. This X-point traversal of C2 provides us a good opportunity to observe and study the physics in the vicinity of the X-point. Figure 2b shows the location of C2 at 09:48:25.637 UT for the magnetic configuration in another plane, as determined by the position of C2 and the A-null as well as the tangential direction of the X-line. The magnetic field connectivity in

Figure 2b reveals that the magnetic field pattern is near the fan surface of the A-null. It is then found that C2 locates near the X-line.

[10] The observations by C2 during passing through the X-line near the null are illustrated in Figure 3. Figure 3a reveals the variation of the plasma electron number density in the time range from 09:48:22.5 to 09:48:28.5 UT, obtained from the spacecraft potential measurements by EFW [*Pedersen et al.*, 2008]. A plasma electron density peak of 0.035 (cm^{-3}) relative to adjacent background is observed in the central reconnection region including electron diffusion region when C2 crossed the X-line as shown in Figure 2a. This electron density hump is consistent with a previous numerical simulation result across a 2-D X point [*Fujimoto*, 2006], and implies temporary trapping in the electron diffusion region [*Karimabadi et al.*, 2007] since it is smaller than the trapped electron density in the magnetic island for a long term [*Chen et al.*, 2007]. Moreover, the Kappa, the magnetic field curvature radius measured in electron gyro radius [*Delcourt et al.*, 1996], is estimated to be in the range of 2.4 to 258.1 (see AM). This result indicates that electrons are trapped in magnetic cusp region. The trapped electrons may be accelerated by parallel electric field and electron pressure gradient to high speed (V_e = 2.6×10^4 km/s) observed as energetic electron beams of 2 keV by PEACE (Figure 3f), on the order of electron Alfvén velocity ($V_{Ae} = 4.6 \times 10^4$ km/s) [*Karimabadi et al.*, 2007] (see AM). The electron pressure gradient is estimated to be 2.5 (mV/m), and thus able to accelerate these electrons to an energy level of 1 keV from the null to the C2 position (see AM). The energetic electrons may be reflected from the magnetic cusp mirrors (see Figure 2a) [*Egedal et al.*, 2005] and lead to the bi-directional energetic beams observed by PEACE as shown in Figure 3f. The electron beams are unstable to excite the high frequency electrostatic waves [*Vaivads et al.*, 2004; *Farrell et al.*, 2002] in the neighbourhood of the null, observed by STAFF with a strong enhancement of the electric field wave power spectrum around the electron plasma frequency shown in Figure 3e. Due to the weak magnetization in the null vicinity, the wave is very likely to be the Langmuir rather than an upper hybrid. During the time period around 09:48:25.637 UT, C2 was close to the null, observed a magnetic field dip as low as 1.2 nT illustrated in Figure 3b, and passed through the neutral sheet shown in Figure 3c. The bipolar Hall electric field component, E_y in GSE, is also measured and varies from −40 to 20 mV/m (Figure 3d). Due to the oblique angle between the current sheet and the x−y plane, Hall electric field should have both components of E_y and E_z in GSE. However, E_z in GSE is not measured.

3. Summary

[11] The magnetic field topology (Figures 1 and 2) and plasma dynamic behaviours (Figure 3) around the magnetic null pair are therefore revealed for the first time, observationally. Based on these facts we suggest a new scenario to describe the electron dynamics near a null in the magnetic null pair region. The electrons are considered to temporarily trapped in the electron diffusion region after convecting from the outside lobe region. The trapped electrons may be accelerated to an energy level 2 keV, near the electron Alfvén speed, by the parallel electric field and observed electron pressure gradient. The energetic electrons reflected from the magnetic cusp mirrors lead to bi-directional energetic electron beams observed, which further stir the high frequency electrostatic waves to scatter the electrons to finally escape, in addition to loss cone angle expansion resulting from the reconnected field line relaxing.

[12] **Acknowledgments.** The work is supported by the National Natural Science Foundation of China (NSFC) under grants 40574078, 40336053, 40436015, 40528005, 40325012, and 40390150, and the Foundation of Major Projects of National Basic Research under contract 2006CB806305, as well as the Beijing Education Project XK100010404. We acknowledge the Cluster CIS, FGM, PEACE, STAFF, EFW and RAPID teams and the Cluster Active Archive.

References

Balogh, A., et al. (2001), The Cluster magnetic field investigation: Overview of in-flight performance and initial results, *Ann. Geophys.*, *19*, 1207.

Birn, J., et al. (2001), Geospace Environment Modelling (GEM) magnetic reconnection challenge, *J. Geophys. Res.*, *106*, 3715.

Cattell, C., et al. (2005), Cluster observations of electron holes in association with magnetotail reconnection and comparison to simulations, *J. Geophys. Res.*, *110*, A01211, doi:10.1029/2004JA010519.

Chen, L.-J., et al. (2007), Observation of energetic electrons within magnetic islands, *Nature Phys.*, *4*, 19–23, doi:10.1038/nphys777.

Cornilleau-Wehrlin, N., et al. (2003), First results obtained by the Cluster STAFF experiment, *Ann. Geophys.*, *21*, 437.

Cowley, S. W. H. (1973), A qualitative study of the reconnection between the Earth's magnetic field and an interplanetary field of arbitrary orientation, *Radio Sci.*, *8*, 903.

Delcourt, D., R. F. Martin, and F. Alem (1996), The centrifugal impulse model of nonadiabatic behavior in a field reversal, *Adv. Space Res.*, *18*(8), 295.

Deng, X. H., and H. Matsumoto (2001), Rapid magnetic reconnection in the Earth's magnetosphere generated by whistler waves, *Nature*, *410*, 557.

Dorelli, J. C., A. Bhattacharjee, and J. Raeder (2007), Separator reconnection at Earth's dayside magnetopause under generic northward interplanetary magnetic field conditions, *J. Geophys. Res.*, *112*, A02202, doi:10.1029/2006JA011877.

Dungey, J. W. (1963), The structure of the exosphere, or adventures in velocity space, in *Geophysics: The Earth's Environment*, edited by C. Dewitt, J. Hieblot, and L. Lebeau, p. 505, Gordon and Breach, New York.

Egedal, J., et al. (2005), In situ discovery of an electrostatic potential, trapping electrons and mediating fast reconnection in the Earth's magnetotail, *Phys. Rev. Lett.*, *94*, 025006.

Escoubet, C. P., M. Fehringer, and M. L. Goldstein (2001), The Cluster mission, *Ann. Geophys.*, *19*, 1197.

Farrell, W. M., M. D. Desch, M. L. Kaiser, and K. Goetz (2002), The dominance of electron plasma waves near a reconnection X-line region, *Geophys. Res. Lett.*, *29*(19), 1902, doi:10.1029/2002GL014662.

Fujimoto, K. (2006), Time evolution of the electron diffusion region and the reconnection rate in fully kinetic and large system, *Phys. Plasmas*, *13*, 072904.

Greene, J. (1988), Geometric properties of three-dimensional reconnecting fields with magnetic nulls, *J. Geophys. Res.*, *93*, 8583.

Greene, J. (1992), Locating three-dimensional roots by a bisect ion method, *J. Comput. Phys.*, *98*, 194.

Gustafsson, G., et al. (2001), First results of electric field and density observations by Cluster EFW based on initial months of operation, *Ann Geophys.*, *19*, 1219.

He, J.-S., et al. (2008), A magnetic null geometry reconstructed from Cluster spacecraft observations, *J. Geophys. Res.*, *113*, A05205, doi:10.1029/2007JA012609.

Henderson, P. D., C. J. Owen, A. D. Lahiff, I. V. Alexeev, A. N. Fazakerley, E. Lucek, and H. Rème (2006), Cluster PEACE observations of electron pressure tensor divergence in the magnetotail, *Geophys. Res. Lett.*, *33*, L22106, doi:10.1029/2006GL027868.

Imada, S., R. Nakamura, P. W. Daly, M. Hoshino, W. Baumjohann, S. Mhlbachler, A. Balogh, and H. Rme (2007), Energetic electron acceleration in the downstream reconnection outflow region, *J. Geophys. Res.*, *112*, A03202, doi:10.1029/2006JA011847.

Johnstone, A. D., et al. (1997), Peace: a Plasma Electron and Current Experiment, *Space Sci. Rev.*, *79*, 351–398.

Karimabadi, H., W. Daughton, and J. Scudder (2007), Multi-scale structure of the electron diffusion region, *Geophys. Res. Lett.*, *34*, L13104, doi:10.1029/2007GL030306.

Lau, Y.-T., and J. M. Finn (1990), Three diemensional kinematic reconnection in the presence of field nulls and closed field lines, *Astrophys. J.*, *350*, 672.
Mozer, F. S., S. D. Bale, and T. D. Phan (2002), Evidence of diffusion regions at a subsolar magnetopause crossing, *Phys. Rev. Lett.*, *89*, 015002.
Øieroset, M., et al. (2001), In situ detection of collisionless reconnection in the Earth's magnetotail, *Nature*, *412*, 414.
Pedersen, A., et al. (2008), Electron density estimations derived from spacecraft potential measurements on Cluster in tenuous plasma regions, *J. Geophys. Res.*, *113*, A07S33, doi:10.1029/2007JA012636.
Priest, E. R., and T. G. Forbes (2000), *Magnetic Reconnection: MHD Theory and Applications*, Cambridge Univ. Press, Cambridge, U. K.
Priest, E. R., and V. S. Titov (1996), Magnetic reconnection at three-dimensional null points, *Philos. Trans. R. Soc. London*, *354*, 2951.
Rème, H., et al. (2001), First multispacecraft ion measurements in and near the Earth's magnetosphere with the identical Cluster ion spectrometry (CIS) experiment, *Ann. Geophys.*, *19*, 1303.
Ricci, P., et al. (2004), Collisionless magnetic reconnection in the presence of a guide field, *Phys. Plasmas*, *11*, 4102, doi:10.1063/1.1768552.
Runov, A., et al. (2003), Current sheet structure near magnetic X-line observed by Cluster, *Geophys. Res. Lett.*, *30*(11), 1579, doi:10.1029/2002GL016730.
Vaivads, A., M. André, S. C. Buchert, J.-E. Wahlund, A. N. Fazakerley, and N. Cornilleau-Wehrlin (2004), Cluster observations of lower hybrid turbulence within thin layers at the magnetopause, *Geophys. Res. Lett.*, *31*, L03804, doi:10.1029/2003GL018142.
Vasyliunas, V. M. (1975), Theoretical models of magnetic field line merging, *Rev. Geophys.*, *13*, 303.
Wygant, J. R., et al. (2005), Cluster observations of an intense normal component of the electric field at a thin reconnecting current sheet in the tail and its role in the shock-like acceleration of the ion fluid into the separatrix region, *J. Geophys. Res.*, *110*, A09206, doi:10.1029/2004JA010708.
Xiao, C. J., et al. (2006), In situ evidence for the structure of the magnetic null in a 3D reconnection event in the Earth's magnetotail, *Nature Phys.*, *2*, 478, doi:10.1038/nphys342.
Xiao, C.-J., et al. (2007), Satellite observations of separator-line geometry of three-dimensional magnetic reconnection, *Nature Phys.*, *3*, 609, doi:10.1038/nphys650.

N. Cornilleau-Wehrlin, CETP, CNRS, 10/12 Avenue de L'Europe, F-78140 Velizy, France.

I. Dandouras and H. Reme, Centre d'Etude Spatiale des Rayonnements, BP 4346, F-31028 Toulouse CEDEX 4, France.

X.-H. Deng, Department of Space Physics, Wuhan University, Wuhan, 430072, China.

M. W. Dunlop, Space Sciences Division, SSTD, Rutherford Appleton Laboratory, Chilton, Oxfordshire, OX11 0QX, UK.

C. P. Escoubet, ESTEC, ESA, Postbus 299, NL-2200, AG Noordwijk, Netherlands.

A. Fazakerley, Department of Space and Climate Physics, Mullard Space Science Laboratory, University College London, Holmbury St. Mary, Dorking, RH5 6NT, UK.

S.-Y. Fu, J.-S. He, Z.-Y. Pu, B. Tan, H. Tian, C.-Y. Tu, S. Yao, and Q.-G. Zong, School of Earth and Space Sciences, Peking University, Beijing, 100871, China. (chuanyitu@pku.edu.cn)

K.-H. Glassmeier, Institut für Geophysik und Meteorologie, Technische Universität Braunschweig, Mendelssohnstrasse 3, Braunschweig D-38106, Germany.

E. Lucek, Space and Atmospheric Physics, Imperial College, London, SW7 2BZ, UK.

Z.-W. Ma, Institute for Fusion Theory and Simulation, Zhejiang University, Hangzhou, 310027, China.

A. Pedersen, Department of Physics, University of Oslo, P.O. Box 1048, Blindern, N-0316 Oslo, Norway.

X.-G. Wang, School of Physics, Peking University, Beijing, 100871, China.

C.-J. Xiao, National Astronomical Observatories, Chinese Academy of Sciences, Beijing, 100012, China.